PROGRESS REPORT OF THE SPECTRAL DECODING BASED EOS WITH ORGANIC POCKELS EO CRYSTALS

Y. Okayasu*, S. Matsubara and H. Tomizawa, JASRI, Sayo-gun, Hyogo 6795198, Japan
K. Ogawa, RIKEN SPring-8 Center, Sayo-gun, Hyogo 6795198, Japan
T. Matsukawa and H. Minamide,
RIKEN Center for Advanced Photonics, Sendai, Miyagi, 9800845, Japan

Abstract

EO signal intensities depending on electron bunch charges were measured with the DAST crystal at EUV-FEL accelerator, SPring-8/SACLA on March and April 2013. Refractive indices and EO coefficients of the crystal are calculated based on experimental conditions and compared with their references. Radiation damage is also quantitatively discussed with measured background level of EO signal intensity spectra which are associated with a static phase retardation based on biaxial natural birefringence of the crystal.

INTRODUCTION

Measurement methods for temporal structure of ultrashort electron bunch has been examined and developed by various kinds of electro-optic sampling (EOS) techniques, such as temporal, spectral and spatial decoding method, at several FEL accelerator facilities since early 2000's. Inorganic Pockels EO crystals have been generally utilized for the EOS.

Conventional EOS with inorganic Pockels crystals, such as GaP or ZnTe, is well known to limit the temporal resolution by 120-210 fs (FWHM), since general inorganic Pockels EO crystals have their unique absorption properties in frequency domain e.g. ∼5 THz for ZnTe and ∼11 THz for GaP [1, 2], which are equivalent to the frequency region of the Coulomb field associated with the electron bunch.

On the other hand, since mid-1980's, organic nonlinear optical materials have been extensively investigated and 4-dimethylamino-N'-methyl-4'-stilbazolium tosylate (DAST), which has fast temporal response in the EO effect, was developed by Okada *et al.* in 1986 [3]. DAST is transparent in visible near to IR wavelength range and absorbent in 0.8-1.3 THz [4].

In SPring-8/SACLA, three dimensional EOS with DAST for a few tens of femtoseconds duration of electron bunch was proposed [5] and R&D was proceeded since 2006. Ultrabroadband THz generation up to 200 THz with the DAST crystal was successfully achieved by Katayama *et al.* [6] utilizing aspects of fast response of DAST and indirectly showed that DAST has temporal response less than a few tens of femtoseconds. In order to realize EOS with femtosecond order of temporal resolution, one octave of linear-chirped probe laser pulse source is also required in addition to the DAST crystal, and we are developing both the laser pulse source and optical components [7].

We introduced the DAST crystal into our EOS system and successfully demonstrated the first observation of the bunch charge distribution at EUV-FEL accelerator (SCSS), SPring-8/SACLA on February 2012 [8]. Through the previous experiment, it is found that the EO signal intensity was gradually decreased as radiation dose around the EO test chamber increased. On March and April 2013, we measured electron bunch charge dependencies on EO signal intensities with 0.5 mm thick DAST crystal in addition to further investigation of the radiation dose issue.

EXPERIMENT

EO signal intensities depending on several electron bunch charges were measured and compared with 0.5 mmt of DAST crystal and 1 mmt of ZnTe crystal at SCSS on March and April 2013.

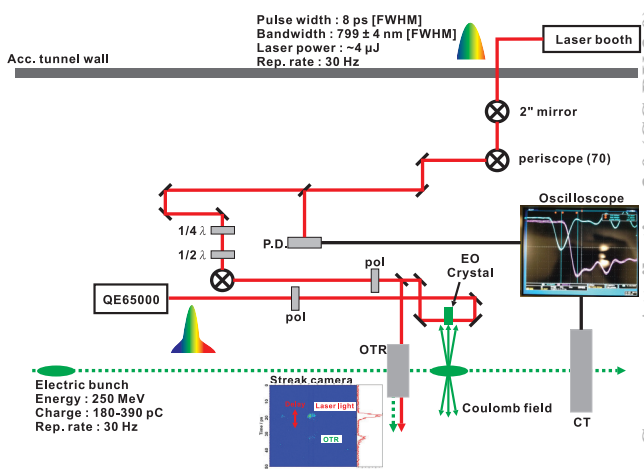

Figure 1: Experimental setup for the DAST EOS.

Experimental setups and accelerator parameters are shown in Fig. 1 and Table 1. Probe laser pulse (pulse width; 8 ps [FWHM], bandwidth; 799 ± 4 nm [FWHM]) was generated in Ti:Sapphire laser source outside the accelerator tunnel, and propagated to an EO chamber located 0.5 m downstream from an OTR monitor. Phase retardation of the incident probe laser was adjusted as 0 degree by a $\lambda/4$ wave plate and its polarization was adjusted to be parallel to a-axis of the DAST crystal (Fig. 2, upper) or

* okayasu@spring8.or.jp

ISBN 978-3-95450-127-4

Table 1: Experimental Parameters of SCSS

Electron bunch	
Energy	250 MeV
Bunch charge	180-390 pC
Bunch duration	350-700 fs (FWHM)
Reputation rate	30 Hz
Peak current	>300 A
Probe laser pulse	
Bandwidth	8 nm (FWHM) @ 799 nm
Pulse energy	~4 μJ (~20 μJ/cm^2)
Pulse width	8 ps (FWHM)
Reputation rate	30 Hz
Chirp rate	0.97 ps/nm (w/ 0.5 mmt DAST)

[-1,1,0] axis of ZnTe by $\lambda/2$ wave plate and the 1st polarizer. Electron bunch (energy; 250 MeV, bunch charge; 190-310 pC) passed through the EO chamber, simultaneously with the probe laser pulse. Incident phase retardation of the probe laser pulse was changed inside the EO crystal due to the birefringence associated with the Coulomb field of the electron bunch. Eventually, ellipsoid polarization components of the probe laser pulse were evaluated and demodulated as a electron bunch charge distribution by the 2nd polarizer (both 1st and 2nd polarizers consist the crossed Nichole configuration) and a spectrometer (Ocean Optics, QE65000).

In the EO chamber, total four Pockels EO crystals and a Ce:YAG phosphor were mounted as shown in Fig. 2 (lower). The Ce:YAG phosphor was used to calibrate electron bunch coordinates and adjust Pockels EO crystals coordinates for the electron bunch. For Pockels EO crystals, one was $3^W \times 4^D \times 1^T$ mm^3 of ZnTe crystal and other three were DAST crystals with different sizes and thicknesses. Fig. 2 (upper) shows one of DAST crystal ($4^W \times 5^D \times 0.5^T$ mm^3) with crystal axis configurations and relative electron bunch coordinates drawings.

Fig. 3 compares typical EO signal intensities measured by the spectrometer for ZnTe ($3^W \times 4^D \times 1^T$ mm^3, left) and DAST ($4^W \times 5^D \times 0.5^T$ mm^3, right). Electron bunch length was ~350 fs (FWHM) and bunch charge were 360 ± 10 pC for ZnTe and 375 ± 10 pC for DAST. For each figure, black-solid curves are directly measured signal intensity spectra, red-solid curves are background spectra without electron bunch and blue-solid ones are their subtractions. In addition, distance between electron bunch center and Pockels EO crystal edge was 1.5 mm for each crystal. One can find EO signal intensity spectrum of the DAST crystal has dips on both sides of major peak, i.e. ~3000 counts of negative offset. This offset is due to static phase retardation components associated with the natural birefringence of biaxial DAST crystal which is equivalent to a background signal and cannot be canceled by crossed polarizers.

Next, peak counts of EO signal intensity spectra (blue-curves) are derived with single-Gaussian fit and compared

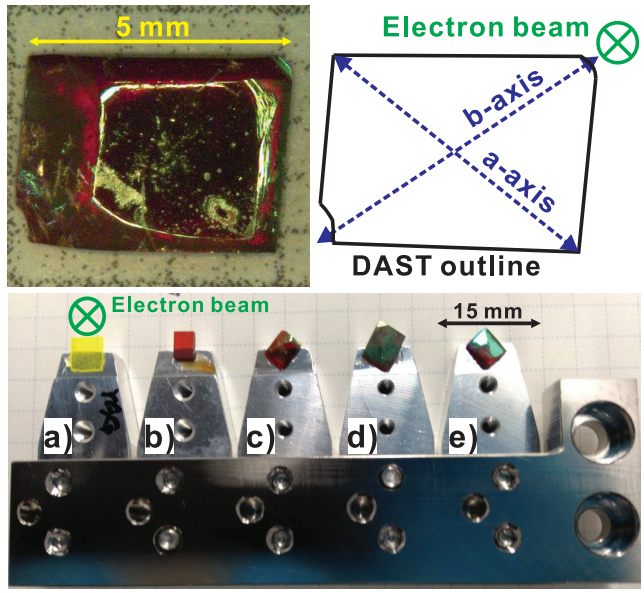

Figure 2: $4^W \times 5^D \times 0.5^T$ mm^3 of the DAST crystal (upper left) and its crystal axes configuration (upper right). Lower shows various crystals mounted on a holder. a) Ce:YAG for fine alignment of crystal position with electron bunch, b) ZnTe (1 mmt) for calibration, c)-d) DAST crystals with different thicknesses and sizes.

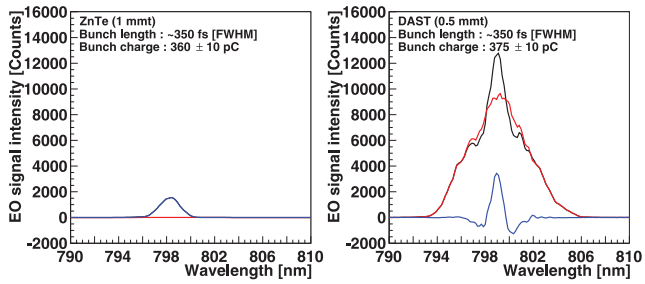

Figure 3: EO signal intensity comparison between ZnTe ($3^W \times 4^D \times 1^T$ mm^3, left) and DAST ($4^W \times 5^D \times 0.5^T$ mm^3, right) in wavelength domain. In each histogram, original spectra measured by the spectrometer are drawn with black curves, red curves are background spectra without electron bunch and blue curves are subtractions of these above. Distance between bunch center and crystal edge was 1.5 mm for each crystal.

in Fig. 4 for ZnTe (left) and DAST (right) crystals changing bunch charge with green plots.

Phase retardation ($\Delta\phi$) of ZnTe and DAST crystals are described as [9];

$$\Delta\phi = \frac{2\pi E n_0^3 r_{41} d}{\lambda} \quad \text{(ZnTe)}, \tag{1}$$

$$\Delta\phi = \frac{\pi E (n_a^3 r_{11} - n_b^3 r_{21}) d}{\lambda} \quad \text{(DAST)}, \tag{2}$$

respectively. d and λ are crystal thickness and wavelength

ISBN 978-3-95450-127-4

of the probe laser pulse, respectively. Refractive indices and EO coefficients for ZnTe (n_0 and r_{41}) and DAST crystals (both a and b-axes; n_a, n_b, r_{11} and r_{21}) at 800 nm are reported as $n_0 = 2.85$ and $r_{41} = 4$ pm/V [1], $n_a = 2.70$, $n_b = 1.89$ [11], $r_{11} = 77 \pm 8$ pm/V and $r_{21} = 42 \pm 5$ pm/V [12], respectively. E is the Coulomb field associated with the electron bunch (bunch charge; q and bunch length; σ in rms);

$$E = \frac{q}{(2\pi)^{3/2}\epsilon_0 r\sigma}\,, \tag{3}$$

where r is distance between electron bunch center and EO crystal edge. Note that, refractive index changes in the EO media can be written by sum of Pockels and Kerr EO effect terms. However, since strength of the electric field from the electron bunch is estimated to be 20-40 MV/m in our experimental condition, Kerr EO effects can be negligible in such higher electric field. EO signal intensity (I) can be expressed by $\sin^2(\Delta\phi/2)$ [10], thus signal intensities for ZnTe and DAST crystals can be described as;

$$I = V_0 \sin^2\left(\frac{\pi E n_0^3 r_{41} d}{\lambda}\right), \tag{4}$$

$$I = V_0 \sin^2\left(\frac{\pi E (n_a^3 r_{11} - n_b^3 r_{21}) d}{2\lambda} + \phi_0\right), \tag{5}$$

respectively. For each equation, V_0 is a free parameter, which depends on the incident probe laser pulse energy, and ϕ_0 is the static phase retardation which is written as;

$$\phi_0 = \frac{2\pi}{\lambda}(n_b - n_a)d\,. \tag{6}$$

In case of 0.5 mm thick DAST crystal and 799 nm of probe laser pulse, ϕ_0 is estimated to be ∼-3200 rad with refractive indices described above.

Measured bunch charge dependencies of EO signal intensities for ZnTe and DAST crystals are shown in Fig. 4 and their calculation results are also overlaid with blue dot-lines as a reference. Calculated refractive indices and EO coefficients based on our experimental conditions for both ZnTe and DAST crystals are listed and compared with references in Table 2. The static phase retardation of the DAST crystal, which was used in our experiment, is estimated to be $\phi_0 = -3200$ rad.

Through a series of our EOS experiments with DAST crystals, it is found that optical characteristics of the DAST crystal are very sensitive for radiation dose. In our former experiment, which held in 2012, the EO signal of a DAST crystal survived only for ∼30 minutes [8]. Decrease of EO signal intensity was also observed through this experiment which held on 2013. We considered that the decrease of the EO signal intensity has consequence with the OTR monitor usage. In Fig. 5, EO signal intensity spectra are compared for the same 0.5 mm thick DAST crystal without (left) and with (right) usage of the OTR monitor which was located ∼0.5 m upstream from the EO chamber. Probe laser pulse energies for both conditions were equivalent. Data taking time was about one hour for each. Total spatial radiation dose was measured with Gafchromic films on the EO

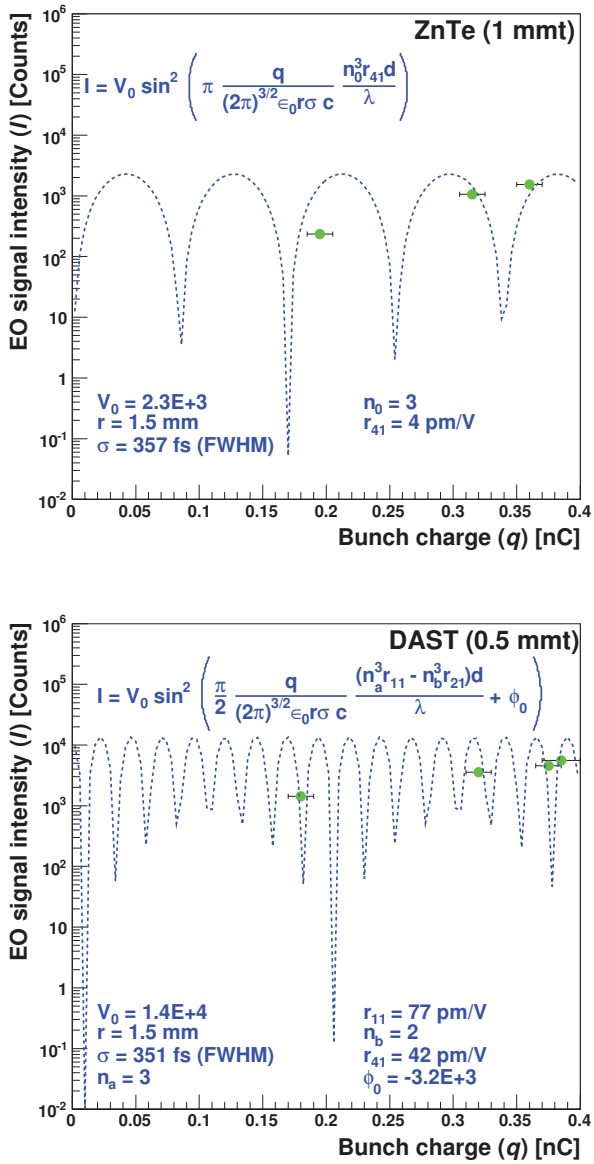

Figure 4: Measured EO signal intensities depending on electron bunch charge (green dots) for ZnTe (1 mmt, upper) and DAST (0.5 mmt, lower). Calculations based on experimental conditions are also overlaid with blue dot-lines as a reference.

chamber and estimated to be 74.6 ± 6.8 Gy (phase 1; Fig. 5, left) and 255.8 ± 66.8 Gy (phase 2; Fig. 5, right). Signal level of the background, which is associated with the static phase retardation described as Eq. (6), is explicitly reduced in phase 2. As far as referring Eq. (6), refractive indices are considered to be changed. As a result, we found that radiation damage for DAST crystals can be controlled and avoided by removing crystals away from the electron bunch orbit in case of the OTR monitor usage.

ISBN 978-3-95450-127-4

Table 2: Calculated Refractive Indices and EO Coefficients Based on the Experimental Conditions for ZnTe and DAST Crystals Comparing to References

	Calculation (λ=799 nm)	References ($\lambda = 800$ nm)
ZnTe		
n_0	3	2.85 [1]
r_{41} [pm/V]	4	4 [1]
DAST		
n_a	3	2.70 [11]
n_b	2	1.89 [11]
r_{11} [pm/V]	77	77 ± 8 [12]
r_{21} [pm/V]	42	42 ± 5 [12]

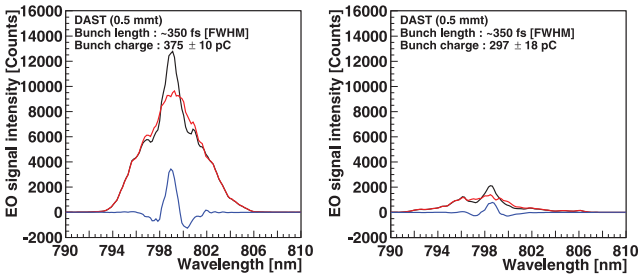

Figure 5: EO signal intensity comparison with 0.5 mm thick DAST crystal between phase 1 (74.6 ± 6.8 Gy) and phase 2 (255.8 ± 66.8 Gy).

SUMMARY AND DISCUSSION

Electron bunch charge dependencies on EO signal intensities were measured and compared with ZnTe ($3^W \times 4^D \times 1^T$ mm^3) and DAST ($4^W \times 5^D \times 0.5^T$ mm^3) crystals by the spectral decoding based EOS at SCSS, SPring-8/SACLA on March and April 2013.

Refractive indices and EO coefficients of both ZnTe and DAST were calculated based on our experimental conditions which are consistent with their references. Much more sufficient statistics of the experimental data are required for further precise discussion about refractive indices and EO coefficients investigation. The static phase retardation of the DAST crystal is also determined for probe laser pulse with central wavelength of 799 nm. This static phase retardation, which never exists in isotropic Pockels EO crystals such as ZnTe and GaP, induces background components on the EO signal intensity spectrum. Thus it is important to control crystal axes configuration not only a and b-axes, but also c-axis during the DAST crystal production process to realize precise EOS. Especially for the direction ambiguity of c-axis may induce conical refraction for the probe laser pulse, which makes the situation more complicated.

The causal relationship between the decrease of the EO signal intensity and the radiation dose was quantitatively investigated and we found that the radiation damage on the DAST crystal can be controlled and avoided by moving the crystal away from the electron bunch while using the OTR monitor. Also, the static phase retardation of the DAST crystal gives important information for radiation damages on the crystal.

For further investigation about the radiation damage issue, we proceed to establish an in-situ measuring system of EO coefficient itself in addition to elements and structure analyses, such as XPS, FT-IF and solid NMR analyses. We also plan to investigate optical properties of DAST crystals with coating techniques for deliquescence property of the crystal, and assembling to ensure the uniformity of crystal axes in wider region of the DAST crystal from November 2013.

REFERENCES

[1] S. Casalbuoni, H. Schlarb, B. Schmidt, P. Schmuser, B. Steffen and A. Winter, Phys. Rev. ST Accel. Beams **11**, 072802 (2008)

[2] G. Berden, W.A. Gillespie, S.P. Jamison, E.-A. Knabbe, A.M. MacLeod, A.F.G van der Meer, P.J. Phillips, H. Schlarb, B. Schmidt, P. Schmuser and B. Steffen, Phys. Rev. Lett. **99**, 164801 (2007)

[3] H. Nakanishi, H. Matsuda, S. Okada and M. Kato, Proc. MRS Int. Mtg. Adv. Mater. **1**, 97 (1989)

[4] M. Walther, K. Jensby, S. R. Keiding, H. Takahashi and H. Ito, Opt. Lett. **25**, 911 (2000)

[5] H. Tomizawa, H. Hanaki and T. Ishikawa, in *Proceedings of the 29th International Free Electron Laser Conference (FEL07), Novosibirsk, Russia*, (2007), p472

[6] I. Katayama, R. Akai, M. Bito, H. Shimosato, K. Miyamoto, H. Ito and M. Ashida, Appl. Phys. Lett. **97**, 021105 (2010)

[7] H. Tomizawa, K. Ogawa, T. Sato, Y. Okayasu, S. Matsubara, T. Togashi, E.J. Takahashi, M. Aoyama, A. Iwasaki, S. Owada, H. Minamide, T. Matsukawa and M. Yabashi, in *Proceedings of the XXVI Linear Accelerator Conference, Tel-Aviv, Israel*, (2012), p657

[8] Y. Okayasu, H. Tomizawa, S. Matsubara, N. Kumagai, A. Maekawa, M. Uesaka and T. Ishikawa, Phys. Rev. Lett. ST Accel. Beams **16**, 052801 (2013)

[9] C. Winnewisser, P. Uhd Jepsen, M. Schall, V. Schyja and H. Helm, Appl. Phys. Lett. **70**, 3069 (1997)

[10] S. Sohma, H. Takahashi, T. Taniuchi and H. Ito, Chem. Phys. **245**, 359, (1999)

[11] P.Y. Han, M. Tani, F. Pan and X.-C. Zhang, Opt. Lett. **25**, 675 (2000)

[12] F. Pan, G. Knöpfle, Ch. Bosshard, S. Follonier and R. Spreiter, Appl. Phys. Lett. **69**, 13 (1996)

ISBN 978-3-95450-127-4